Colloids and Surfaces B: Biointerfaces 158 (2017) 76–83

Contents lists available at ScienceDirect

Colloids and Surfaces B: Biointerfaces

journal homepage: www.elsevier.com/locate/colsurfb

Protocols

Interaction of acylated and unacylated forms of *E. coli* alpha-hemolysin with lipid monolayers: a PM-IRRAS study

Romina F. Vázquez[a], María A. Daza Millone[b], Felippe J. Pavinatto[c,1], Vanesa S. Herlax[a], Laura S. Bakás[d], Osvaldo N. Oliveira Jr.[c], María E. Vela[b], Sabina M. Maté[a,*]

[a] *Instituto de Investigaciones Bioquímicas de La Plata (INIBIOLP), CCT- La Plata, CONICET. Facultad de Ciencias Médicas. Universidad Nacional de La Plata, 60 y 120, 1900, La Plata, Argentina*
[b] *Instituto de Investigaciones Fisicoquímicas Teóricas y Aplicadas (INIFTA), CCT- La Plata, CONICET. Universidad Nacional de La Plata, Sucursal 4 Casilla de Correo 16, 1900, La Plata, Argentina*
[c] *Instituto de Física de São Carlos (IFSC), Universidade de São Paulo, SP, Brazil*
[d] *Centro de Investigación de Proteínas Vegetales (CIPROVE), Departamento de Ciencias Biológicas, Facultad de Ciencias Exactas. Universidad Nacional de La Plata. 47 y 115, 1900, La Plata, Argentina*

ARTICLE INFO

Article history:
Received 24 February 2017
Received in revised form 12 June 2017
Accepted 19 June 2017
Available online 24 June 2017

Keywords:
HlyA toxin
PM-IRRAS
Langmuir monolayers
Acylated proteins
Protein-membrane interactions

ABSTRACT

Uropathogenic strains of *Escherichia coli* produce virulence factors, such as the protein toxin alpha-hemolysin (HlyA), that enable the bacteria to colonize the host and establish an infection. HlyA is synthetized as a protoxin (ProHlyA) that is transformed into the active form in the bacterial cytosol by the covalent linkage of two fatty-acyl moieties to the polypeptide chain before the secretion of HlyA into the extracellular medium. The aim of this work was to investigate the effect of the fatty acylation of HlyA on protein conformation and protein-membrane interactions. Polarization-modulated infrared reflection-absorption spectroscopy (PM-IRRAS) experiments were performed at the air-water interface, and lipid monolayers mimicking the outer leaflet of red-blood-cell membranes were used as model systems for the study of protein-membrane interaction. According to surface-pressure measurements, incorporation of the acylated protein into the lipid films was faster than that of the nonacylated form. PM-IRRAS measurements revealed that the adsorption of the proteins to the lipid monolayers induced disorder in the lipid acyl chains and also changed the elastic properties of the films independently of protein acylation. No significant difference was observed between HlyA and ProHlyA in the interaction with the model lipid monolayers; but when these proteins became adsorbed on a bare air-water interface, they adopted different secondary structures. The assumption of the correct protein conformation at a hydrophobic-hydrophilic interface could constitute a critical condition for biologic activity.

1. Introduction

Virulence factors are produced by uropathogenic strains of *Escherichia coli* that enable the bacteria to colonize, break the host defense barriers, invade, and disseminate, to cause severe infections [1]. One of the main virulence factors is the 110-kDa protein toxin alpha-hemolysin (HlyA), it considered the prototype member of the RTX toxin family of Gram negative bacteria [2]. HlyA is synthetized as a protoxin (ProHlyA) that is transformed into the active form in the bacterial cytosol before secretion. This posttranslational modification consists in the amide-linkage of fatty-acyl moieties to the ε-amino groups of two internal lysine residues [3,4]. Once the lipidic modification occurs—and after toxin secretion into the extracellular medium—the binding of Ca^{2+} ions to the C-terminus of the protein confers full lytic and cytotoxic activity to the bacterial toxin [5,6]. Many mammalian cell types—including red blood cells, myeloid and lymphoid cells, and renal epithelial cells—are attacked by HlyA [7–10]. The precise mechanism by which this acylated protein exerts these well characterized toxic effects is unclear, though protein-membrane interactions are known to play a critical role because cell membranes are the primary target of the toxin. After the initial adsorption to the cell membrane, the insertion of the protein into the hydrophobic matrix is postulated to yield dynamic proteolipidic pores in the lipid bilayer [11–13]. Different cell responses are triggered by toxin-membrane interactions, par-

* Corresponding author at: INIBIOLP, CCT– La Plata, CONICET, Facultad de Ciencias Médicas, Universidad Nacional de La Plata. 60 y 120, 1900, La Plata, Argentina.
E-mail addresses: smate@med.unlp.edu.ar, mate.sabina@gmail.com (S.M. Maté).
[1] Current permanent address: Clean Energy Institute, University of Washington, WA, Seattle, USA.

http://dx.doi.org/10.1016/j.colsurfb.2017.06.020
0927-7765/

ticularly a massive Ca^{2+} ion entry into the cells, producing an ionic imbalance that eventually leads to osmotic cell lysis [14,15].

In contrast to HlyA, the toxin precursor ProHlyA has no lytic or cytotoxic effects [16]. Rather, fatty acylation appears to favor an irreversible binding of the toxin to the target-cell membrane to promote protein–protein interactions that result in oligomerization and pore formation [13]. Early studies on hemolytic activity revealed that both HlyA and ProHlyA bind to the same extent to the erythrocyte membranes, though only HlyA produces cell lysis [3,17]. In a recent study, we demonstrated that ProHlyA also induces early morphologic transitions in rabbit erythrocytes, thus suggesting that the interaction of either form of the toxin with the erythrocyte membrane may initially perturb the lipid bilayer causing a discocyte-to-echinocyte morphologic transition in response to protein binding, independently of Ca^{2+} influx. Nevertheless, only when erythrocytes are exposed to HlyA, does the onset of Ca^{2+} entry, triggered by the acylated toxin, occur to produce swelling and cell lysis [18].

In this study, we further investigated the effect of HlyA acylation by determining the interaction of the acylated and unacylated forms of HlyA with lipid monolayers mimicking the outer leaflet of red-blood-cell membranes [19]. Surface-pressure measurements and determinations of polarization-modulated infrared reflection-absorption spectroscopy (PM-IRRAS) measurements revealed that the behavior of both proteins is similar in terms of the structural changes induced in the monolayers, but that those interactions do not explain the differences in toxicity between the two forms of the toxin. When, however, pure protein monolayers were analyzed, different secondary-structural elements were found to be exposed at the air-water interface, with the entire HlyA polypeptide chain being more extended than its unacylated counterpart. Thus, the assumption of the correct protein conformation at a hydrophobic-hydrophilic interface could constitute a critical condition for biologic activity.

2. Materials and methods

2.1. Materials

HlyA and ProHlyA were purified from culture filtrates of the *E. coli* strains WAM 1824 [20] and WAM 783 [21], respectively, following the procedure described in [22]. The lipids 1,2-dioleoyl-sn-glycero-3-phosphocholine (DOPC), N-palmitoyl-D-erythro-sphingosylphosphorylcholine (16:0-SM), and cholesterol (Chol) were purchased from Avanti Polar Lipids (Birmingham, AL, USA) and used without further purification. Tris buffer, NaCl, $CaCl_2$, and other reagents, all analytical-grade, were acquired from Sigma–Aldrich (St. Louis, MO, USA) unless otherwise stated. Chloroform and methanol, HPLC-grade, were purchased from Merck (Darmstadt, Germany). The surface tension and resistivity of the ultrapure water used were 72.2 mN/m and 18.2 MΩ cm at 23 °C, respectively.

2.2. Surface-pressure experiments

Surface-pressure (π) measurements were carried out with a Langmuir trough by a NIMA Model 102A instrument (NIMA Technology, Coventry, UK) with a Wilhelmy platinum plate as the π sensor. The aqueous subphase consisted of 20 mM Tris, 150 mM NaCl, 2 mM $CaCl_2$, pH 7.4 (TBS Buffer) prepared in ultrapure water. For protein-insertion assays, the ternary lipid mixture of DOPC/16:0-SM/Chol at a 2:1:1 molar ratio dissolved in chloroform was gently spread over the subphase until the desired initial surface pressure (πo) was attained. After solvent evaporation and πo stabilization (5 min), HlyA or ProHlyA from stock solution prepared in TBS Buffer were injected into the bulk of the subphase with a Hamilton microsyringe at a final concentrations of 20 nM, and the increment in π ($\Delta\pi$) was recorded over time. The same experimental set up was used to evaluate the surface-active properties of the proteins by analyzing their adsorption kinetics in the absence of lipids. Curves of $\Delta\pi$ *vs* t were fitted according to Eq. (1), from which $\Delta\pi eq$ (maximum $\Delta\pi$ achieved under equilibrium conditions) and τ (the time needed to reach half of $\Delta\pi eq$) were obtained at various πo values of the Langmuir films.

$$\Delta\pi = \Delta\pi eq\, t/(\tau + t) \quad (1)$$

Isotherms of π-Area were obtained for DOPC/16:0-SM/Chol monolayers and HlyA- or ProHlyA-DOPC/16:0-SM/Chol mixed monolayers. The procedure stated in brief: The ternary lipid mixture dissolved in chloroform was spread onto the surface of the teflon trough (NIMA 102A) filled with TBS Buffer as the subphase. After solvent evaporation and monolayer relaxation (5 min), the films were isometrically compressed at 5 $cm^2\ min^{-1}$. For obtaining mixed protein-lipid monolayers, the proteins were injected into the subphase beneath the lipid monolayer (at concentrations of 1 or 4 nM protein). After protein adsorption onto the interface (10 min) compression isotherms were obtained as stated above. Areas per lipid molecule in $Å^2$ were calculated considering only the lipid molecules present at the interface. The in-plane elasticity of the films was analyzed by calculating the compressibility modulus (Cs^{-1}) from the π-Area isotherms according to Eq. (2) [23]:

$$Cs^{-1} = -A(\partial\pi/\partial A) \quad (2)$$

where A represents the area per lipid molecule at the surface pressure π. All the surface pressure measurements were performed at 23 ± 1 °C.

The compression isotherms were all repeated at least three times to ensure the reproducibility of the measurements, with standard deviations lower than 5%.

2.3. Measurements of polarization-modulated infrared reflection-absorption spectroscopy measurements

PM-IRRAS measurements were performed with a KSV PMI 550 instrument (KSV, Biolin Scientific Oy, Espoo, Finland). The experimental setup used was similar to that described by Pavinatto et al. [24]. In the PM-IRRAS technique, the incoming light is continuously modulated between *s*- and *p*-polarization at a high frequency, so that the spectra for the two polarizations can be measured simultaneously. Therefore, the polarized reflectivities for the directions parallel (Rp) and perpendicular (Rs) to the plane of incidence are both measured and the differential reflectivity spectrum $\Delta R = (Rp - Rs)/(Rp + Rs)$ is obtained. Since absorption of the *p*-polarized light comes mainly from vertically oriented dipoles, while that of the *s*-polarized light arises from the horizontally oriented ones, the difference between the two spectra provides information on the orientation of the vibrational dipoles, which is surface-specific since the molecules in the subphase and nearby vapor phase have random orientations. The angle of incidence of the light beam was 80°, at which orientation positive bands indicate a transition moment oriented on the surface plane, whereas negative bands indicate an orientation perpendicular to the surface. An average of 600 scans was collected for each spectrum at a resolution of 8 cm^{-1}. The spectra of the monolayer were divided by that of the subphase to produce the resulting normalized PM-IRRAS spectra. All the experiments were carried out in a class 10,000 clean room at 23 ± 1 °C.

For the acquisition of PM-IRRAS spectra of proteins at the air-water interface, so-called *Gibbs monolayers* were obtained by adsorption of the proteins (20 nM) to the interface after their injection into the bulk subphase (TBS Buffer), and 10 min after the

injection PM-IRRAS spectra were collected. The monolayers were then further compressed and spectra obtained at 25 and 30 mN/m.

In order to analyze protein-lipid interactions, lipid monolayers were obtained by spreading the lipid mixture of DOPC/16:0-SM/Chol (2:1:1 molar ratio) dissolved in chloroform on the subphase (TBS Buffer) surface. After solvent evaporation and monolayer relaxation, the monolayers were compressed at 5 $cm^2.min^{-1}$ until a lateral pressure of 30 mN/m was attained. Then HlyA or ProHlyA were injected from the stock solutions into the bulk of the subphase (10 nM protein final concentration) and PM-IRRAS spectra were collected 15 min after the addition of the proteins. The lateral pressure of the monolayers was maintained constant at 30 mN/m during the whole procedure.

Representative PM-IRRAS spectra of two (for protein monolayers) or three (for protein-lipid–interaction measurements) independent experiments are shown.

3. Results and discussion

3.1. Adsorption of HlyA and ProHlyA onto the air-water interface

HlyA is a surface-active molecule that causes the water surface tension to decrease, as measured in a Langmuir balance [25]. The surface activity of the toxin has been attributed mainly to amphipathic α-helices within the N-terminal domain, though the C-terminal region has also been reported to contribute [25,26]. Fig. 1 illustrates the time courses of the adsorption of HlyA and ProHlyA to the air-water interface, where similar $\Delta\pi$ values were observed after injection of the proteins into the aqueous subphase. The total $\Delta\pi$ measured after 10 min was ~17 mN/m for 80 or 40 nM of protein injected, whereas an increment of ~15 mN/m was obtained for 20 nM. The adsorption thus occurred with fast kinetics at these concentrations, reaching a stable signal by only 4 min after HlyA or ProHlyA injection.

3.2. Protein monolayers at the air-water interface

Acylation plays a key role in promoting the association of proteins to membranes [27]. Nevertheless, additional binding contributions are needed to stably anchor a protein—and especially large proteins like HlyA (at 110 kDa)—to a membrane [28]. HlyA and ProHlyA both bind to erythrocyte membranes, thus indicating that the polypeptide chain itself has an affinity for the lipid bilayer [13,29]. Considering that different arrangements of HlyA and ProHlyA at the membrane surface may determine the final protein activity, we performed studies on pure protein monolayers at the air-water interface. The crystalline structure of HlyA has not yet been resolved, though data obtained from circular-dichroism spectra have revealed that this protein of 1023 amino acids contains a 36% of α-helix structure in aqueous solution [6]. Indeed, ten amphipathic α-helices have been identified in the toxin's amino-acid sequence located at the N-terminal half of the protein—at least, according to structural-prediction methods [30]. Regarding the secondary structure at the C-terminus, the HlyA amino-acid sequence contains—as do other members of the RTX toxin family—arrays of Gly- and Asp-enriched repetitions that adopt β-sheet structures and form a β-parallel roll; as reported for the alkaline protease of *Pseudomona aeruginosa*, it being another member of this toxin family [31]. Finally, the two acylation sites—Lys 563 and 689—are located in the central region of the polypeptide chain. Fig. 2, Panel A presents a schematic illustration of the HlyA structure.

In order to analyze the conformation adopted by these proteins at an air-water interface, we collected PM-IRRAS spectra of pure protein monolayers. For this purpose, the proteins (20 nM) were injected into the bulk subphase and left for 10 min to adsorb onto the interface. At this time point, the increments in π obtained for HlyA and ProHlyA were 16 and 18 mN/m, respectively, and the initial PM-IRRAS spectra were measured at these π values. Both of the protein monolayers were then further compressed up to 25 and 30 mN/m and the IRRAS spectra collected at those π levels as well. Panels B and C in Fig. 2 illustrate the spectra for each protein at the different π values, featuring the amide-I (1700–1600 cm^{-1}) and amide-II (1600–1500 cm^{-1}) bands. The amide-I band contains contributions mainly from the C=O stretching mode with a minor contribution from C—N, thus providing useful information for the analysis of protein secondary structure [32]. The examination of this region for HlyA revealed that the active protein exposed both α-helix (1659 cm^{-1}) and β-sheet structures (1629 cm^{-1}) when adsorbed at the air-water interface (Fig. 2, Panel B). The deconvolution of the amide-I band obtained for HlyA at 16 mN/m indicated that 80% of this band corresponded to the α-helix component and 20% to β-sheet structures (*inset* in Fig. 2, Panel B). In the amide-II region—it corresponding mainly to the N—H bending modes—three major bands were observed in HlyA spectra at low surface pressures—located at 1536, 1578, and 1516 cm^{-1}—that could be assigned to α-helix (1536 and 1578 cm^{-1}) and random coil structures (1516 cm^{-1}), respectively [33].

A different profile of bands was observed in the ProHlyA spectra (Fig. 2, Panel C). The strong band in the amide-I region of the protoxin could be assigned mainly to α-helices located at the interface (1654 cm^{-1}), whereas no appreciable bands could be detected in the 1630 cm^{-1} region of β-sheet structure as opposed to HlyA, although a slight shoulder at 1688 cm^{-1} could be assigned to the presence of antiparallel β-sheets (*inset* in Fig. 2, Panel C). The amide-II region for ProHlyA contained bands at 1536 and 1570 cm^{-1}, that could be assigned to α-helical structures.

With progressive compression of the protein monolayers, the protein surface concentration increased, resulting in an increment in the IRRAS-signal intensity. During compression, no major changes were observed with respect to the shape of the amide-I band; and similar proportions of the secondary structure appeared at both low and high surface pressures, which correspondence indicated that both proteins maintained their conformation at the air-water interface during compression.

3.3. Protein adsorption onto lipid monolayers

Membrane model systems provide valuable insights into the properties of complex biologic membranes and enable the study of protein-membrane interactions under controlled conditions. Lipid monolayers at the air-water interface represent the most simplified model resembling one half of the cell membrane [34].

The interaction of HlyA and ProHlyA was therefore investigated for monolayers of DOPC/16:0-SM/Chol at a 2:1:1 molar ratio and various initial surface pressures πo. This ternary-lipid mixture represents a composition similar to that found in the outer leaflet of mammalian erythrocyte membranes [35,36]. The injection of either protein into the subphase produced an increase in surface pressure indicating protein insertion into the lipid monolayer, as shown in Fig. 3, panels A and B. The greater the πo, the lower the incorporation of the proteins into the monolayer (*i. e.*, manifest as a lower $\Delta\pi$) because of the closer packing of the lipids at higher initial surface pressures. These curves of $\Delta\pi$ *vs.* time were fitted to Eq. (1), from which function the time (τ) needed to achieve half of the maximum $\Delta\pi$ was obtained. Panel C of Fig. 3 indicates a faster kinetics for HlyA, as manifest in lower τ values that were essentially independent of πo. In contrast, with ProHlyA, τ increased progressively with increments in πo, thus indicating a strong dependence of the association rate on the packing density of the lipid molecules at the interface.

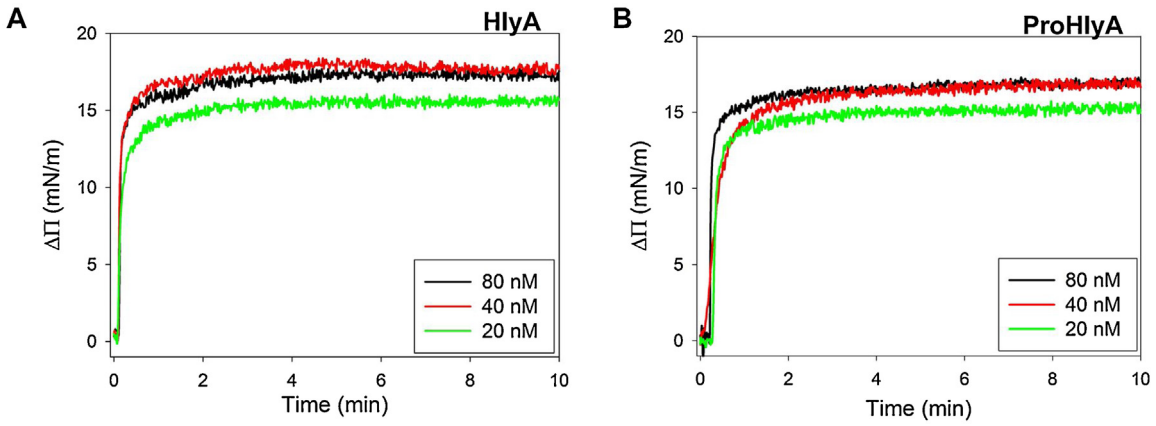

Fig. 1. Surface-activity of HlyA and ProHlyA. Adsorption kinetics of HlyA (Panel A) and ProHlyA (Panel B) to the air–water interface measured with a Langmuir balance at 23 ± 1 °C. Protein solutions were injected into the bulk of the subphase (TBS buffer) in order to reach the desired concentrations, and the increments in surface pressure ($\Delta\pi$) were recorded over time.

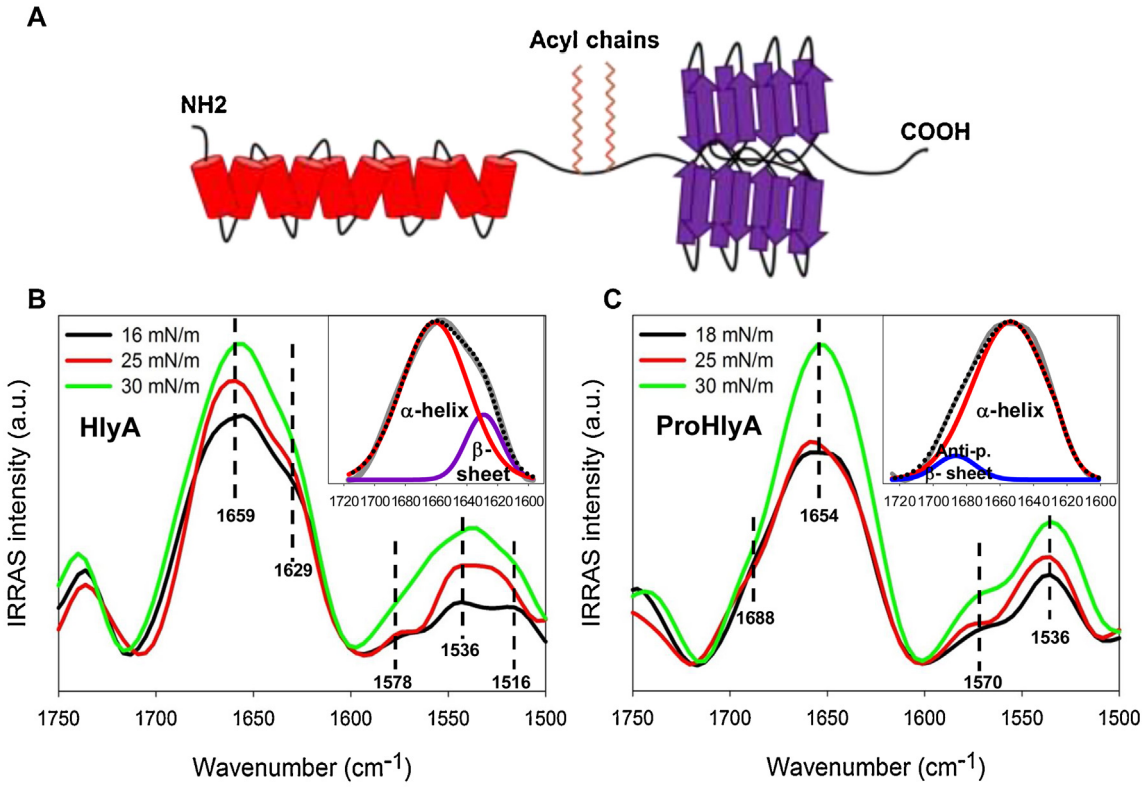

Fig. 2. HlyA and ProHlyA secondary structure at the air-water interface. Panel A: Schematic illustration of HlyA structure. The α-helices are represented as red cylinders and the β-sheet structures as violet arrows. Panels B and C: Amide-I (1700–1600 cm^{-1}) and Amide-II (1600–1500 cm^{-1}) regions of the PM-IRRAS spectra of HlyA (Panel B) or ProHlyA (Panel C) monolayers at different compression levels at the air-water interface. The Gibbs monolayers were obtained by adsorption of the proteins (20 nM) to the interface after their injection into the bulk of the subphase (TBS Buffer). At 10 min after the injection, PM-IRRAS spectra were collected—the curves corresponding to 16 (black, Panel A) and 18 (black, Panel B) mN/m in the figures for HlyA and ProHlyA, respectively. The monolayers were then further compressed and the spectra were obtained at 25 (red) and 30 (green) mN/m. The *insets* in Panels B and C depict the deconvoluted amide-I band of the HlyA monolayer at 16 mN/m and the ProHlyA monolayer at 18 mN/m, respectively. There, the bands assigned to α-helical (red) and β-sheet (violet) as well as those assigned to antiparallel β-sheet structures (blue) are indicated, and the dotted curve corresponds to the sum of the intensities of the different secondary-structure bands. Fourier self-deconvolution was used to perform the band assignments. (For interpretation of the references to colour in this figure legend, the reader is referred to the web version of this article.)

Also worth noting is that the total $\Delta\pi$ at equilibrium ($\Delta\pi eq$) was slightly higher for ProHlyA, as demonstrated in the plots in Panel D of Fig. 3, from which lines the so-called *exclusion surface pressure* or *critical pressure* (πc) could be determined by extrapolating the plots to zero $\Delta\pi eq$. This parameter represents the πo above which no further incorporation of proteins into the monolayer takes place. A higher πc was obtained for ProHlyA (27.9 ± 0.4 mN/m) compared to HlyA (22.2 ± 0.3 mN/m), suggesting an increased capacity of ProHlyA over HlyA for insertion into membranes. This difference is indeed paradoxical in view of ProHlyA's complete lack of lytic activity. The monolayer studies clearly reveal that insertion and lysis are two conceptually and experimentally different phenomena. The results obtained here reinforced the notion that different protein arrangements are inserting into the lipid monolayers, with ProHlyA structures being favored over those of HlyA, although with slower kinetics compared to those of the active toxin. For both proteins,

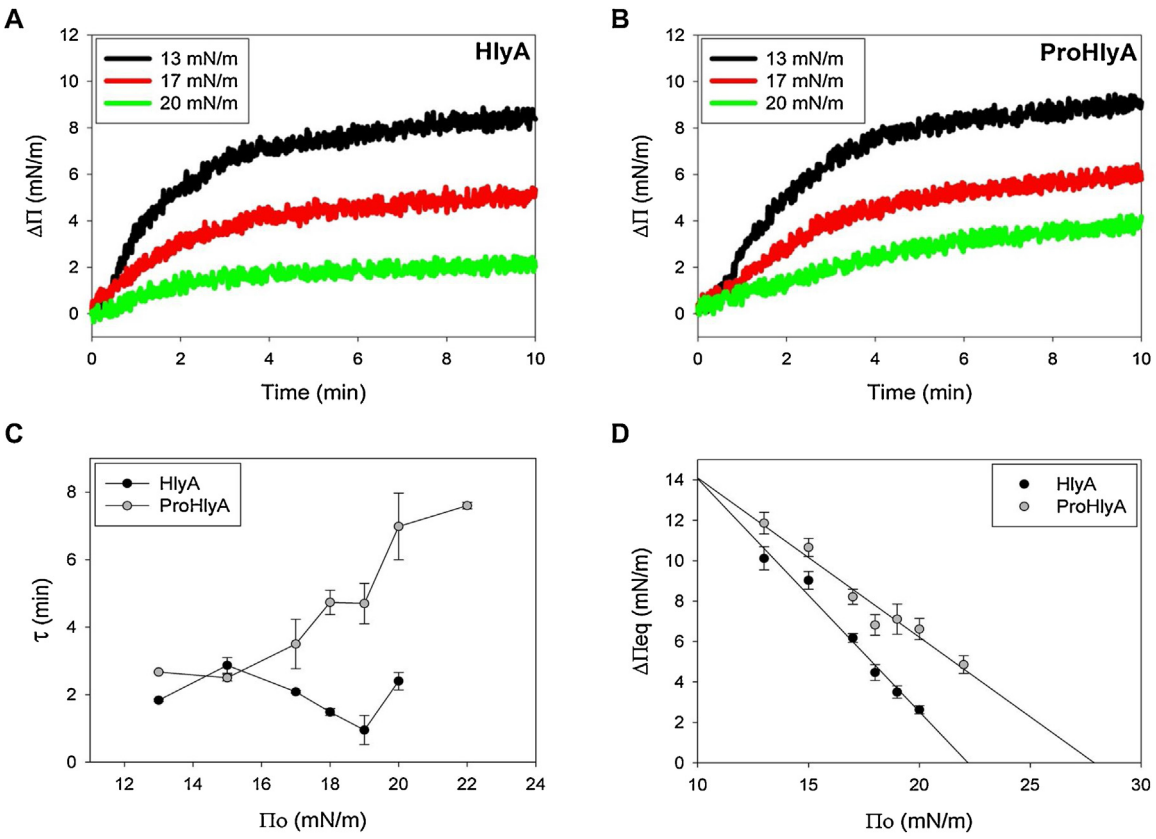

Fig. 3. *Protein interaction with lipid monolayers.* Kinetics of insertion of HlyA (Panel A) or ProHlyA (Panel B) into lipid monolayers of DOPC/16:0-SM/Chol at a 2:1:1 molar ratio. The ternary lipid mixture was spread over the subphase (TBS buffer) to achieve the initial surface pressures indicated in the figures [πo values of 13 (black curve), 17 (red), and 20 (green) mN/m]. After solvent evaporation (5 min), the proteins were injected from stock solutions to give a final protein concentration of 20 nM in the subphase and the increase in surface pressure ($\Delta\pi$) was monitored over time. Measurements were performed at 23 ± 1 °C. Panel C: the time (τ) needed to achieve half of $\Delta\pi eq$ is plotted as a function of πo for each protein. Curves of $\Delta\pi$ *vs time* obtained at each πo were fitted to Eq. (1) (cf. Materials and Methods Section), and τ as well as the $\Delta\pi$ attained at equilibrium ($\Delta\pi eq$) were calculated. Panel D: the plots show the $\Delta\pi eq$ obtained for the interaction of either protein with the lipid films at different πo values. The exclusion surface pressure for each protein was obtained from these plots by extrapolating the curves to $\Delta\pi eq = 0$. The values represent the mean ± standard deviations. (For interpretation of the references to colour in this figure legend, the reader is referred to the web version of this article.)

the exclusion pressure occurred at π values higher than the equilibrium surface pressure of the proteins alone (cf. Fig. 1), indicating that these proteins were stabilized at the interface by interaction with the monolayer lipids. Because these exclusion pressures are lower than the pressure believed to correspond to the packing in real cell membranes (viz 30–35 mN/m [29]), one could assume that the proteins should not penetrate a biologic membrane, especially HlyA. Nevertheless, the membranes occurring in nature are highly dynamic structures where lateral-pressure values fluctuate, and thus these proteins must still be able to find appropriate conditions for insertion *in vivo* [37].

3.4. Compression isotherms

In order to evaluate the effect of protein incorporation into the lipid monolayers, we performed compression isotherms of DOPC/16:0-SM/Chol monolayers (2:1:1 molar ratio) and of mixed films obtained by the addition of HlyA or ProHlyA (at 1 or 4 nM protein concentration). Fig. 4 depicts the π-Area isotherms (Panel A) and the compressibility modulus (Cs^{-1}) calculated from those isotherms at different π (Panel B)—Cs^{-1} values were calculated assuming that the protein molecules incorporated into the lipid film at low surface pressure remained at the interface during the compression process. Neat DOPC/16:0-SM/Chol monolayers exhibited a liquid-expanded profile with Cs^{-1} values remaining below 100 mN/m, in agreement with results reported previously [19]. In the mixed monolayers, an expansion to higher areas—calculated as the total monolayer area divided by the number of lipid molecules initially spread at the interface—was observed (Panel A) that could be accounted for by the monolayer disturbance resulting from the incorporation of the proteins into the lipid films. This alteration was higher at 4 nM of HlyA or ProHlyA since more protein molecules must have been incorporated into the lipid films than at 1 nM; in fact, the initial adsorption of the proteins to the interface before compression already produced an increment of ~13 mN/m in π when either protein was added at 4 nM. The presence of HlyA or ProHlyA produced a decrease in the Cs^{-1} values over the entire range of π, thus indicating that the proteins changed the elastic properties of the monolayers, making the films more fluid. At a protein concentration of 4 nM, a maximum in Cs^{-1} was observed at ~15–18 mN/m similar to the values obtained for pure protein monolayers (Fig. S1 in the Supplementary Material). These observations suggested that the proteins exerted a predominant influence over the interfacial characteristics of the mixed monolayers at this protein concentration.

3.5. PM-IRRAS measurements

Interactions between guest molecules and Langmuir monolayers can be probed with PM-IRRAS, which technique permits the analysis of lipid conformational order and the secondary structure of proteins plus their orientation [33]. Figs. 5 and 6 present the PM-IRRAS spectra for monolayers at a lateral pressure of 30 mN/m of neat DOPC/16:0-SM/Chol and after the addition of HlyA

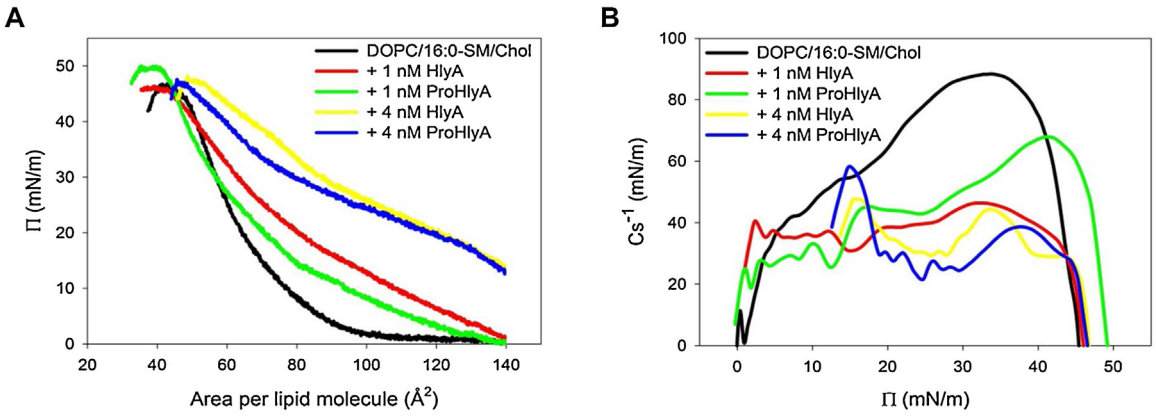

Fig. 4. *Effect of HlyA and ProHlyA incorporation into lipid monolayers.* Panel A: Compression isotherms of DOPC/16:0-SM/Chol monolayers (2:1:1 molar ratio) and of HlyA- and ProHlyA-DOPC/16:0-SM/Chol mixed monolayers. In the figure, the surface pressure π is plotted as a function of the areas per lipid—calculated as Å^2/lipid molecule without considering the protein molecules adsorbed at the monolayer. Panel B: The compressibility modulus Cs^{-1}, calculated for each treatment from those isotherms according to Eq. (2), is plotted on the *ordinate* as a function of the surface pressure π in mN/m on the *abscissa*.

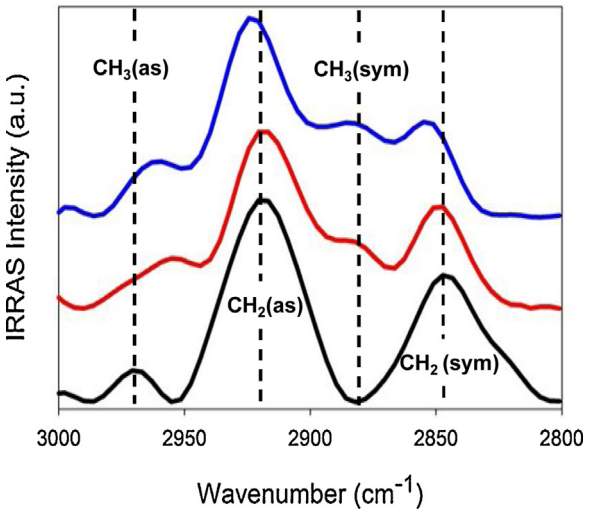

Fig. 5. *Acyl-chain conformational changes induced by HlyA and ProHlyA.* The 2800–3000 cm^{-1} region of the PM-IRRAS spectra of neat DOPC/16:0-SM/Chol (2:1:1 molar ratio) monolayers at a lateral pressure of 30 mN/m is the black record. The same measurements were performed at 15 min after the addition of HlyA (red) or ProHlyA (blue) into the subphase (at a 10 nM final concentration). The lateral pressure of the monolayers was maintained at 30 mN/m after toxin incorporation. The bands corresponding to the CH_2 and the CH_3 antisymmetric (as) and symmetric (sym) stretching modes are indicated in the figure. Measurements were performed at 23 ± 1 °C. (For interpretation of the references to colour in this figure legend, the reader is referred to the web version of this article.)

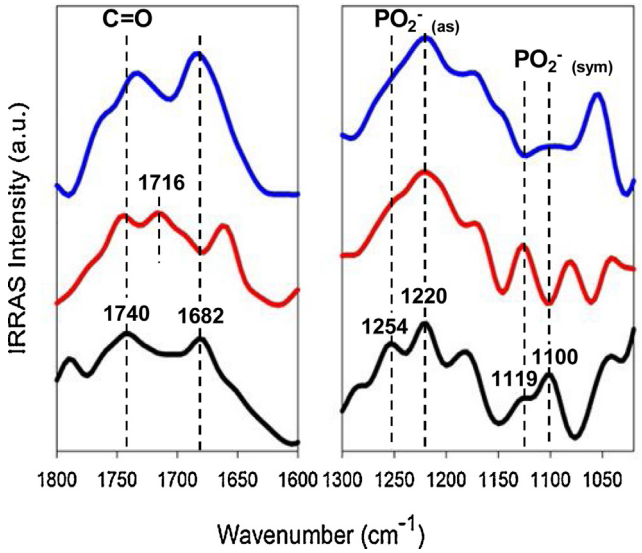

Fig 6. *Changes in the carbonyl and phosphate regions.* PM-IRRAS spectra were obtained for neat DOPC/16:0-SM/Chol (2:1:1 molar ratio) monolayers at a lateral pressure of 30 mN/m (black record). The same measurements were performed 15 min after the addition of HlyA (red) or ProHlyA (blue) into the subphase (at a 10 nM final concentration). The lateral pressure of the monolayers was maintained at 30 mN/m after protein addition. Measurements were performed at 23 ± 1 °C. The main carbonyl and phosphate bands are indicated in the figure. (For interpretation of the references to colour in this figure legend, the reader is referred to the web version of this article.)

or ProHlyA. The packing and orientation of the lipid alkyl chains can be monitored by analyzing the C—H stretching bands in the 3000–2800 cm^{-1} region of the spectra [38]. The two main bands centered at 2916 and 2847 cm^{-1} for DOPC/16:0-SM/Chol monolayer in Fig. 5 were assigned to CH_2 antisymmetric and symmetric stretching modes, respectively. At the frequencies observed these bands are indicative of a relatively ordered acyl-chain conformation [39]. A band assigned to CH_3 antisymmetric stretching mode at 2969 cm^{-1} was also detected. The CH_2 bands were affected slightly by the presence of HlyA and ProHlyA, which alteration also induced shifts in the antisymmetric CH_3 bands (to 2955 cm^{-1} and 2959 cm^{-1} for HlyA and ProHlyA, respectively). Furthermore—and most significantly—bands at 2882 cm^{-1} (for HlyA) and 2881 cm^{-1} (for ProHlyA) assigned to symmetric CH_3 stretching appeared, which modification represents a strong indication of increased disorder in the lipid films after protein addition.

PM-IRRAS spectra of neat DOPC/16:0-SM/Chol monolayers contained well defined, intense CH_2 bands, whereas no peaks corresponding to the symmetric CH_3-stretching mode could be detected. When HlyA or ProHlyA were incorporated into the subphase, the lipid acyl chains became less ordered than in the pure-lipid monolayers, as indicated by the appearance of CH_3 symmetric bands [40]. Furthermore, shifts in the CH_2 bands to higher wavenumbers were also observed, especially after ProHlyA incorporation; a feature that is also indicative of an increased disorder in the lipid acyl chains as a result of the protein-lipid interactions since hydrocarbon chains containing *gauche* conformers absorb IR radiation at higher frequencies than those containing *all-trans* configurations [38].

In the interfacial region, the C=O and PO_2—-stretching vibrations are sensitive to the local environment and are influenced by hydrogen bonding [41]. For the lipid films, a band centered at

~1740 cm^{-1} was assigned to C=O stretching mode along with a second band at ~1682 cm^{-1} that may be attributed to the amide group of SM (Fig. 6, left panel). There, in the spectra of HlyA (red record), bands at ~1744 and 1716 cm^{-1} were observed corresponding to the nonhydrated and hydrated C=O vibrations, respectively [42]. In the ProHlyA-containing monolayers (blue record), the band assigned to C=O stretching appeared at 1732 cm^{-1}. For both proteins, the band originally at 1682 cm^{-1} remained, but it was shifted to lower wavenumbers in the presence of HlyA. With respect to the PO_2^--stretching vibrations (Fig. 6, right panel), two bands (~1254, 1220 cm^{-1}) were observed in the lipid-monolayer spectrum corresponding to the PO_2^- antisymmetric stretching and a band at 1100 cm^{-1} with a shoulder at 1119 cm^{-1} for the symmetric stretching. In the presence of either protein, a change in the shape of the spectra was observed and a broad band encompassing the 1254 cm^{-1} band appeared with a maximum at ~1220 cm^{-1}. In the 1100 cm^{-1} region two bands were observed at 1126 and 1080 cm^{-1} after HlyA addition, while an intense band at 1053 cm^{-1} and a weak one at 1095 cm^{-1} appeared in the presence of ProHlyA.

In the analysis of the contribution of the proteins to the PM-IRRAS signal, the protein-amide bands (Amide I 1700–1600 cm^{-1} and Amide II 1600–1500 cm^{-1}) were not clearly identified because of the interference caused by the water-bending vibration, which reflected in a strong and broad "dip" seen in the curves at around 1600 cm^{-1} for all three monolayers. These observations, in combination with the low exclusion pressures determined (cf. Fig. 3, Panel D), reinforced the idea of an interfacial interaction of both proteins with the lipid monolayers at 30 mN/m. Furthermore, the results demonstrated that the adsorption of HlyA or ProHlyA to the lipid monolayers produced changes in the accessibility of water to the phosphates and C=O groups of the phospholipids. The changes observed in the CH region of the spectra after protein addition (cf. Fig. 5) indicated that, even though the proteins did not insert into this lipid monolayer at 30 mN/m, their interaction with the polar headgroups of the phospholipids produced a decrease in the hydrocarbon-chain packing.

In summary, the data obtained here indicate that both the acylated and unacylated proteins have similar surface properties. In addition, except for the faster association kinetics of the acylated protein, no major differences were observed in the interaction of the proteins with the DOPC/16:0-SM/Chol monolayers. The πc values determined from the adsorption kinetics (Fig. 3, Panel D) as well as the PM-IRRAS measurements indicated that both proteins may interact superficially with the model cell membrane, also introducing a conformational disorder in the lipid acyl chains. Soluble proteins that bind to the membrane—*e. g.* HlyA—interact by a combination of electrostatic and hydrophobic forces, initially adsorbing onto the phospholipid headgroups and then penetrating partially or totally the hydrophobic-hydrophilic interface. Within this context, our results indicate that the fatty-acyl moieties are not critical for protein adsorption onto lipid monolayers, an event that introduces disorder in the lipid acyl chains and changes in the elastic properties of the films. These effects could trigger the morphologic transitions reported in erythrocytes after treatment with either HlyA or ProHlyA [18], but do not account for the differences in toxicity between the proteins. In spite of these similarities between the two forms of HlyA, the PM-IRRAS measurements revealed that the secondary-structural elements exposed at the air-water interface were different for the two proteins. In this regard, the results indicated that α-helices in the N-terminal region along with β-sheets in the C-terminus of the polypeptide chain were present at the air-water interface upon adsorption of HlyA, whereas the α-helical structures prevailed at the interface with ProHlyA. Early reports exploring the conformations of these proteins in aqueous solution had indicated that HlyA presents a more flexible configuration while ProHlyA adopts a more compact structure, suggesting that the fatty acids covalently bound to HlyA were involved in the adoption of an active molten-globule conformation [43]. In line with these considerations, our results (Fig. 2, panels B and C) suggest that, when the acylated protein reaches the interface from the subphase, HlyA's polypeptide chain is exposed to a greater extent than ProHlyA's.

The differences observed by PM-IRRAS in protein conformation (Fig. 2, panels B and C) at a hydrophobic-hydrophilic interface may have a profound impact on the interactions of the toxin with biologic membranes. For instance, glycophorin, a glycoprotein present in the erythrocyte membrane, has been postulated to be a putative receptor for the toxin in those cells facilitating the lytic effect of HlyA [44]. The region binding to glycophorin has been localized at the C-terminal end of the protein (amino acids 914–936) [45]. The exposure of the C-terminal domain at a hydrophobic interface would locate the glycophorin binding region close to the cell membrane. On the contrary, if the binding region to glycophorin is not exposed, as could occur in the instance of ProHlyA (Fig. 2, Panel C), the binding to this erythrocyte receptor would be prevented. Furthermore, since the entire HlyA polypeptide chain was found to be more extended at the interface (Fig. 2, Panel B), we can infer that the acyl chains could also be exposed. This exposure may contribute to the irreversible anchoring of the active toxin to the target-cell membrane in an adequate conformation to trigger the transductional pathways needed for toxin activity, events that have not been observed for the unacylated protein [18,29].

4. Conclusion

HlyA is a virulence factor frequently expressed by uropathogenic *E. coli* strains associated with the development of severe urinary-tract infections. For this reason, HlyA, as many toxins, constitutes a potential vaccine target. Nevertheless, despite its having been studied for many years, the mechanism of action of HlyA and its function in infection remain elusive. Results obtained in this work through the use of lipid Langmuir monolayers as membrane model systems suggest that the presence of the fatty-acyl moieties favors the kinetics of association of the protein, but is not a critical element involved in the interaction with ternary monolayers resembling the outer leaflet of erythrocyte membranes. Our findings suggest that the exposure of the main protein domains of HlyA, when located at the interface, could play a relevant role in the stable anchoring and toxic activity of the protein by facilitating protein–protein interactions between toxin monomers and/or membrane receptors. These findings provide new insights into the protein-membrane interactions involved in early stages in the contact of both the virulent HlyA and the inactive ProHlyA with erythrocyte model membranes, thus contributing to an understanding of the mechanism of action of these large proteins. A further characterization of this mechanism could lead to the development of therapeutic treatments for the associated urinary-tract infections as well as contribute to a much wider area of investigation since other members of the RTX-toxin family are produced by a variety of human pathogens.

Acknowledgements

We thank Mario Raúl Ramos for the graphic designs. This work was supported by the Agencia Nacional de Promoción Científica y Tecnológica [grant number PICT 2657/2013], the Comisión de Investigaciones Científicas de la Provincia de Buenos Aires (CICBA), the Universidad Nacional de La Plata [grant number M11/181], and FAPESP [grant number 2013/14262-7] and CNPq (Brazil). R.V. is a post-doctoral fellow of the Consejo Nacional de Investigaciones Científicas y Técnicas (CONICET), Argentina. L.B., M.E.V., and S.M.

are members of the Carrera del Investigador CICBA, Argentina. M.A.DM. and V.H. are members of the Carrera del Investigador of CONICET. Dr. Donald F. Haggerty, a retired academic career investigator and native English speaker, edited the final version of the manuscript.

Appendix A. Supplementary data

Supplementary data associated with this article can be found, in the online version, at http://dx.doi.org/10.1016/j.colsurfb.2017.06.020.

References

[1] T.J. Wiles, R.R. Kulesus, M.A. Mulvey, Exp. Mol. Pathol. 85 (1) (2008) 11–19.
[2] T.J. Wiles, M.A. Mulvey, Future Microbiol. 8 (1) (2013) 73–84.
[3] P. Stanley, L.C. Packman, V. Koronakis, C. Hughes, Science 266 (5193) (1994) 1992–1996.
[4] P. Stanley, V. Korornakis, C. Hughes, Microbiol. Mol. Biol. Rev. 62 (1998) 309–333.
[5] H. Ostolaza, A. Soloaga, F.M. Goñi, Eur. J. Biochem. 228 (1) (1995) 39–44.
[6] L. Bakás, M. Veiga, A. Soloaga, H. Ostolaza, F. Goñi, Biochim. Biophys. Acta 1368 (2) (1998) 225–234.
[7] J.M. DeBoy, I.K. Wachsmuth, B.R. Davis, J. Clin. Microbiol. 12 (2) (1980) 193–198.
[8] S.J. Cavalieri, I.S. Snyder, Infect. Immun. 36 (2) (1982) 455–461.
[9] S. Bhakdi, M. Muhly, S. Korom, G. Schmidt, J. Clin. Invest. 85 (1990) 1746–1753.
[10] P. Uhlen, A. Laestadius, T. Jahnukainen, T. Soderblom, F. Backhed, G. Celsi, H. Brismar, S. Normark, A. Aperia, A. Richter-Dahlfors, Nature 405 (6787) (2000) 694–697.
[11] L. Bakas, H. Ostolaza, W.L. Vaz, F.M. Goñi, Biophys. J. 71 (4) (1996) 1869–1876.
[12] L. Bakas, A. Chanturiya, V. Herlax, J. Zimmerberg, Biophys. J. 91 (10) (2006) 3748–3755.
[13] V. Herlax, S. Mate, O. Rimoldi, L. Bakas, J. Biol. Chem. 284 (37) (2009) 25199–25210.
[14] S. Sanchez, L. Bakas, E. Gratton, V. Herlax, PLoS One 6 (6) (2011) pe21127.
[15] M. Skals, N.R. Jorgensen, J. Leipziger, H.A. Praetorius, Proc. Natl. Acad. Sci. U. S. A. 106 (10) (2009) 4030–4035.
[16] A. Soloaga, H. Ostolaza, F. Goñi, F. de la Cruz, Eur. J. Biochem. 238 (2) (1996) 418–422.
[17] M.E. Bauer, R.A. Welch, Infect. Immun. 64 (11) (1996) 4665–4672.
[18] R.F. Vázquez, S.M. Maté, L.S. Bakás, C. Muñoz-Garay, V.S. Herlax, Biochim. Biophys. Acta 1858 (8) (2016) 1944–1953.
[19] S.M. Mate, R.F. Vazquez, V.S. Herlax, M.A. Daza Millone, M.L. Fanani, B. Maggio, M.E. Vela, L.S. Bakas, Biochim. Biophys. Acta 1838 (7) (2014) 1832–1841.
[20] M. Moayeri, R.A. Welch, Infect. Immun. 65 (6) (1997) 2233–2239.
[21] D.F. Boehm, R.A. Welch, I.S. Snyder, Infect. Immun. 58 (6) (1990) 1959–1964.
[22] R.F. Vazquez, S.M. Mate, L.S. Bakas, M.M. Fernandez, E.L. Malchiodi, V.S. Herlax, Biochem. J 458 (3) (2014) 481–489.
[23] G.L. Gaines, Insoluble Monolayers at Liquid-Gas Interfaces, Interscience Publishers, New York, 1966.
[24] F.J. Pavinatto, C.P. Pacholatti, É.A. Montanha, L. Caseli, H.S. Silva, P.B. Miranda, T. Viitala, O.N. Oliveira, Langmuir 25 (17) (2009) 10051–10061.
[25] L. Sanchez-Magraner, A.L. Cortajarena, F.M. Goni, H. Ostolaza, J. Biol. Chem. 281 (9) (2006) 5461–5467.
[26] L. Sanchez-Magraner, A.R. Viguera, M. Garcia-Pacios, M.P. Garcillan, J.L. Arrondo, F. de la Cruz, F.M. Goñi, H. Ostolaza, J. Biol. Chem. 282 (16) (2007) 11827–11835.
[27] M.D. Resh, Prog Lipid Res 63 (2016) 120–131.
[28] C.T. Pool, T.E. Thompson, Biochemistry 37 (28) (1998) 10246–10255.
[29] V. Herlax, L. Bakas, Chem. Phys. Lipids 122 (1–2) (2003) 185–190.
[30] A. Soloaga, M.P. Veiga, L.M. Garcia-Segura, H. Ostolaza, R. Brasseur, F.M. Goñi, Mol. Microbiol. 31 (4) (1999) 1013–1024.
[31] U. Baumann, S. Wu, K.M. Flaherty, D.B. McKay, EMBO J. 12 (9) (1993) 3357–3364.
[32] D.M. Byler, H. Susi, Biopolymers 25 (3) (1986) 469–487.
[33] A. Blume, A. Kerth, Biochim. Biophys. Acta 1828 (10) (2013) 2294–2305.
[34] H. Brockman, Curr. Opin. Struct. Biol. 9 (4) (1999) 438–443.
[35] B. Engelmann, S. Streich, U.M. Schönthier, W.O. Richter, J. Duhm, Biochim. Biophys. Acta 1165 (1) (1992) 32–37.
[36] S. Mate, J.V. Busto, A.B. Garcia-Arribas, J. Sot, R. Vazquez, V. Herlax, C. Wolf, L. Bakas, F.M. Goñi, Biophys. J. 106 (12) (2014) 2606–2616.
[37] L.A. Bagatolli, O.G. Mouritsen, Front. Plant Sci. 4 (2013) p457.
[38] R. Mendelsohn, J.W. Brauner, A. Gericke, Annu. Rev. Phys. Chem. 46 (1995) 305–334.
[39] R.G. Snyder, A.L. Aljibury, H.L. Strauss, H.L. Casal, K.M. Gough, W.F. Murphy, J. Chem. Phys. 81 (12) (1984) 5352–5361.
[40] C.L. Leverette, R.A. Dluhy, Colloids Surf. A 243 (1–3) (2004) 157–167.
[41] W. Hübner, A. Blume, Chem. Phys. Lipids 96 (1–2) (1998) 99–123.
[42] A. Blume, W. Hubner, G. Messner, Biochemistry 27 (21) (1988) 8239–8249.
[43] V. Herlax, L. Bakas, Biochemistry 46 (17) (2007) 5177–5184.
[44] A.L. Cortajarena, F.M. Goñi, H. Ostolaza, J. Biol. Chem. 276 (16) (2001) 12513–12519.
[45] A.L. Cortajarena, F.M. Goñi, H. Ostolaza, J. Biol.Chem 278 (21) (2003) 19159–19163.